DMD Fast Forward. Published on July 8, 2011 as doi:10.1124/dmd.111.040840

Significant Species Difference in Amide Hydrolysis of GDC-0834, a Novel Potent and Selective Bruton's Tyrosine Kinase (BTK) Inhibitor

Lichuan Liu, Jason S. Halladay, Young Shin, Susan Wong, Melis Coraggio, Hank La, Matthew Baumgardner, Hoa Le, Sashi Gopaul, Jason Boggs, Peter Kuebler, John C. Davis, Jr, X. Charlene Liao, Joseph W. Lubach, Alan Deese, C. Gregory Sowell, Kevin S. Currie, Wendy B. Young, S. Cyrus Khojasteh, Cornelis E.C.A. Hop and Harvey Wong

Departments of Drug Metabolism and Pharmacokinetics (L.L., J.S.H., Y.S., S.W., M.C., H.L., M.B., H.L., S.G., J.B., S.C.K., C.E.C.A.H., H.W.), Pharmacokinetics and Pharmacodynamic Sciences (P.K.), Immunology & Experimental Medicine (J.C.D.), Early Development (X.C.L.), Small Molecule Pharmaceutical Sciences (J.L., A.D., C.G.S.), and Medicinal Chemistry (W.B.Y.), Genentech Inc, 1 DNA Way, South San Francisco, CA 94080, USA

Department of Medicinal Chemistry (K.S.C.), CGI Pharmaceuticals Inc, 36 East Industrial Road, Branford, CT 06405, USA

Running Title: Amide hydrolysis in human

Correspondence: Dr. Lichuan Liu

Genentech, Inc.

1 DNA Way, MS# 412a

South San Francisco, CA 94080

E-mail: liu.lichuan@gene.com

TEL: 650-225-4845

FAX: 650-467-3487

Text: 23 pages

Abstract: 247 words

Introduction: 406 words

Discussion: 1500 words

Tables: 4

Figures: 7

References: 31

Abbreviations: RA, rheumatoid arthritis; BTK, Bruton's tyrosine kinase; LM, liver microsomes; NADPH, reduced form of nicotinamide adenine dinucleotide phosphate; PK, pharmacokinetics; MLP, maximum life span; IND, investigational new drug; LC/MS, liquid chromatography/mass spectrometry; K_m, Michaelis-Menten constant; V_{max}, maximum formation rate; GDC-0834, *R*-*N*-(3-(6-(4-(1,4-dimethyl-3-oxopiperazin-2-yl)phenylamino)-4-methyl-5-oxo-4,5-dihydropyrazin-2-yl)-2-methylphenyl)-4,5,6,7-tetrahydrobenzo[*b*]thiophene-2-carboxamide; EDTA: ethylenediaminetetraacetic acid

DMD Fast Forward. Published on July 8, 2011 as DOI: 10.1124/dmd.111.040840
This article has not been copyedited and formatted. The final version may differ from this version.

ABSTRACT

GDC-0834 is a potent and selective inhibitor of Bruton's tyrosine kinase (BTK) investigated as a potential treatment for rheumatoid arthritis (RA). *In vitro* metabolite identification studies in hepatocytes revealed predominant formation of an inactive metabolite (M1) via amide hydrolysis in human. The formation of M1 appeared to be NADPH-independent in human liver microsomes. M1 was found in only minor to moderate quantities in plasma from preclinical species dosed with GDC-0834. Human clearance predictions using various methodologies resulted in estimates ranging from low to high. In addition, GDC-0834 exhibited low clearance in PXB chimeric mice with humanized liver. Uncertainty in human pharmacokinetic prediction and high interest in a BTK inhibitor for clinical evaluation prompted an IND strategy where GDC-0834 was rapidly advanced to a single dose human clinical trial. GDC-0834 plasma concentrations in humans were below the limit of quantitation (< 1 ng/mL) in most samples from the cohorts dosed orally at 35 mg and 105 mg. In contrast, substantial plasma concentrations of M1 were observed. In human plasma and urine, only M1 and its sequential metabolites were identified. The formation kinetics of M1 was evaluated in rat, dog, monkey and human liver microsomes in the absence of NADPH. The maximum rate of M1 formation (V_{max}) was substantially higher in human compared with other species. In contrast, the Michaelis-Menten constant (K_m) was comparable among species. Intrinsic clearance (V_{max}/K_m) of GDC-0834 from M1 formation in human was 23 - 169 fold higher than observed in rat, dog and monkey.

DMD Fast Forward. Published on July 8, 2011 as DOI: 10.1124/dmd.111.040840
This article has not been copyedited and formatted. The final version may differ from this version.

INTRODUCTION

Bruton's tyrosine kinase (BTK) is a member of the Tec family of non-receptor tyrosine kinases, which is expressed in all cells of hematopoietic lineage except plasma cells, natural killer cells and T lymphocytes (Satterthwaite and Witte, 2000; Brunner et al., 2005). BTK is activated by phosphatidylinositol 3-kinase-dependent plasma membrane recruitment and phosphorylation on tyrosine 551 by the Src-family kinase Lyn. Once activated, BTK induces phospholipase C γ2- and Ca^{2+} -dependent signaling leading to the activation of nuclear factor κB- and nuclear factor of activated T cell-dependent pathways (Niiro and Clark, 2002). In B cells, BTK is important for B cell antigen receptor-, CD40- and Toll-like receptor 4-mediated activation and proliferation (Khan et al., 1995). Furthermore, BTK plays a role in B cell antigen processing and presentation (Sharma et al., 2009). Importantly, BTK is also essential in Fcγ receptor -mediated inflammatory cytokine production [tumor necrosis factor α, interleukin (IL)-1β and IL-6] in monocytes/macrophages and therefore can contribute to immune-complex-induced disease (Di Paolo et al., 2011).

The critical roles of BTK in the development, differentiation and proliferation of B-lineage cells have been well-documented (Pan, 2008). The recent discovery of selective inhibitors for BTK has provided convincing evidence that BTK is an attractive target for the treatment of rheumatoid arthritis (RA) and B cell–related diseases, such as lupus, lymphoma and leukemia (Pan et al., 2007; Uckun et al., 2007; Di Paolo et al., 2011, Liu et al., 2011). However, there are currently no approved specific BTK inhibitors on the market. GDC-0834 is a highly selective, reversible, ATP competitive small molecule inhibitor of BTK being developed as a therapeutic for RA (Liu et al., 2011). In

B cells, this compound effectively blocks B cell antigen receptor - and CD40-mediated activation and proliferation. In monocytes, it potently inhibits immune-complex mediated inflammatory cytokine production, including tumor necrosis factor α, which may also contribute to disease pathogenesis in RA.

Preliminary *in vitro* metabolite identification studies of GDC-0834 suggested significant differences in the major route of metabolism in human compared to other preclinical species. In human, an aniline metabolite (M1) formed via an amide hydrolysis reaction appeared to be more predominant when compared to other preclinical species tested. The objective of this study was to characterize the species differences in the metabolism of GDC-0834 in mouse, rat, dog, monkey and human using both *in vitro* and *in vivo* methodologies. An additional objective was to characterize GDC-0834 in a novel humanized liver mouse (PXB) model.

DMD Fast Forward. Published on July 8, 2011 as DOI: 10.1124/dmd.111.040840
This article has not been copyedited and formatted. The final version may differ from this version.

MATERIALS AND METHODS

Materials and Animals

GDC-0834 (Figure 1A) and its aniline metabolite M1 (Figure 1B) were provided by Genentech (South San Francisco, CA, USA) and CGI Pharmaceuticals (Branford, CT, USA). The preclinical *in vivo* studies described herein were conducted according to protocols approved by the IACUC at Genentech (South San Francisco, CA, USA), SRI International (Menlo Park, CA, USA), Covance Laboratories (Madison, WI, USA) or PhoenixBio (Higashi-Hiroshima, Japan). HPLC-grade solvents (acetonitrile, methanol, and water) were purchased from EDM Chemicals, Inc. (Gibbstown, NJ, USA). Formic Acid was purchased from Mallinckrodt, Inc. (Phillipsburg, NJ, USA).

In vivo Preclinical Pharmacokinetics (PK)

GDC-0834 was dosed at 1 mg/kg intravenously (IV) and 5 mg/kg orally (PO) in female CD-1 mouse (n = 24 per route, 3/timepoint), male Sprague–Dawley rat (n = 3 per route) (Charles River Laboratories; Hollister, CA, USA), male beagle dog (n = 3 per route), and male cynomolgus monkey (n = 3 per route) (Covance; Cumberland, VA, USA). For all studies involving oral administration, animals were fasted overnight until 4 h post-dose. Water was supplied ad libitum. The blood samples were collected up to 24 hours post-dose into tubes containing ethylenediaminetetraacetic acid (EDTA) as an anticoagulant. Blood samples were centrifuged within 30 min of collection and plasma was harvested. Plasma samples were stored at approximately −70°C until analysis for both GDC-0834 and its aniline metabolite M1 (PO groups only for M1) by liquid chromatography tandem mass spectrometry (LC/MS/MS, see details in the bioanalytical section). Pharmacokinetic (PK) analysis was performed on either mean plasma

concentration–time data (mouse) or the individual plasma concentration-time data (rat, dog and monkey). PK parameters were estimated by non-compartmental methods using WinNonlin® Enterprise, version 5.2 (Pharsight Corporation; Mountain View, CA, USA). The IV-Bolus input model (Model 201) was used for the IV-dosed group of GDC-0834, and the Extravascular input model (Model 200) was used for the PO-dosed group of GDC-0834 and M1 data.

In vivo PK in PXB Mice with Humanized Livers

PXB-mice (PhoenixBio; Higashi-Hiroshima, Japan) were produced by transplanting human hepatocytes (BD Biosciences; Woburn, MA, USA) into the spleen of 2- to 4-week old male uPA$^{+/+}$/Severe Combined Immunodeficiency Disease (SCID) mice under diethylether anesthesia. After transplantation, mice with a blood human albumin concentration of 7.0 mg/mL or more were selected as PXB-mice for use. GDC-0834 was dosed at 1 mg/kg IV and 5 mg/kg PO in both male PXB and control SCID (Charles River Japan; Kanagawa, Japan) mice. In the IV groups, one animal per group was sacrificed for sampling at 0.033, 0.167, 0.5, 1, 3 and 6 hours post dose. In the PO groups, one animal per group was sacrificed for sampling at 0.083, 0.25, 0.5, 1, 3 and 6 hours post dose. A minimum of 300 μL of blood was collected from each animal via the heart into sodium heparin-coated syringes after which the animals were sacrificed by cardiac puncture and exsanguination. Blood samples were stored on ice until centrifugation within 30 min to obtain plasma. GDC-0834 and M1 metabolite plasma concentrations were assessed using LC/MS/MS. PK parameters were determined by non-compartmental methods as described above.

Liver Microsome and Hepatocyte Metabolic Stability Assays

Metabolic stability assays in liver microsomes were conducted with pooled female CD-1 mouse (n > 10), male Sprague-Dawley rat (n = 20), male Beagle dog (n =3), male Cynomolgus monkey (n = 4) (Celsis In Vitro Technologies; Baltimore, MD, USA) and mixed male and female human (n = 15) (CellzDirect; Durham, NC, USA) liver microsomal incubations. The general assay conditions are described as follows. Incubation mixtures consisted of liver microsomes (0.5 mg microsomal protein/mL), GDC-0834 (1.0 μM) with or without NADPH (1.0 mM) in the potassium phosphate buffer (KPi; 100 mM; pH 7.4) with a final incubation volume of 0.25 mL. Reactions were initiated by the addition of NADPH or buffer and shaken in a water bath open to the air at 37°C. At times 0, 20, 40, and 60 minutes, aliquots (50 μL) were removed and added to termination mixtures (100 μL) containing acetonitrile and an internal standard from in house project. The samples were then centrifuged for 10 minutes at 2,000 x g. The supernatant (90 μL) was removed, combined with 180 μL of water, and analyzed by LC/MS/MS.

Metabolic stability assays in hepatocytes were conducted using cryopreserved pooled female CD-1 mouse (n > 10), male Sprague-Dawley rat (n > 10), male Beagle dog (n = 3), male Cynomolgus monkey (n = 3) and mixed male and female human (n = 10) hepatocytes (CellzDirect; Durham, NC, USA). Vials of hepatocytes were thawed rapidly in a water bath set at 37°C, then diluted with Dulbecco's Modified Eagle's Medium (DMEM; pH 7.4). Cells were isolated by centrifugation, pooled and resuspended in DMEM at 1.0 million viable cells/mL. Membrane integrity of the cells was assessed by trypan blue exclusion. GDC-0834 was dissolved in dimethylsulfoxide at a final

concentration of 10 mM. This GDC-0834 stock was diluted further to 2 μM in DMEM (125 μL) prior to the addition of an equal volume of the 1.0 million cells/mL cell suspension. GDC-0834 (final incubation concentration of 1.0 μM with 0.1% dimethylsulfoxide) and cells (final concentration of 0.5 million cells/mL) were incubated at 37°C in a 95% air/5% CO_2 atmosphere for 3 hours. Aliquots (50 μL) were removed at 0, 1, 2, and 3 hours and added to termination mixtures (100 μL) containing acetonitrile and an internal standard from in house project. The samples were then centrifuged for 10 minutes at 2,000 x g. The supernatant (90 μL) was removed, combined with 180 μL of water, and analyzed by LC/MS/MS.

In vitro Metabolite Identification in Hepatocytes

Metabolite identification studies were performed using cryopreserved pooled female CD-1 mouse (n > 10), male Sprague-Dawley rat (n > 10), male Beagle dog (n = 3), male Cynomolgus monkey (n = 3) and mixed male and female human (n = 10) hepatocytes (CellzDirect; Durham, NC, USA). Briefly, GDC-0834 (10 μM) hepatocyte incubations were conducted in 96-well plates containing approximately 125,000 cells/well in an incubator at 37°C with 5% CO_2 and 95% humidity. Samples from the incubations (100 μL) were taken at 0 and 3 hour time points. Reactions were quenched with 200 μL acetonitrile. Metabolite identification was performed using LC/MS/MS, which consisted of a LC-10AD pump (Shimadzu Corporation; Columbia, MD, USA), a HTS PAL autosampler (CTC Analytics; Carrboro, NC, USA) and a QTRAP®4000 mass spectrometer equipped with a TurboIonSpray® (Applied Biosystems; Foster City, CA, USA). Data-dependent ion, product ion, precursor ion, neutral loss, and multiple-reaction monitoring scans in positive ion electrospray mode

were used to characterize GDC-0834 and its metabolites. The ultraviolet (UV) traces obtained were used to quantify the amount of metabolites formed in hepatocytes relative to GDC-0834 at 0 hour.

Formation Kinetics of M1 Metabolite

Enzyme kinetics studies of M1 formation were performed (MDS Pharma Services; Bothell, WA, USA) using pooled liver microsomes from mixed male and female human, male Cynomolgus monkey, male Beagle dog, and male Sprague-Dawley rat. Briefly, GDC-0834 concentrations of 0.156, 0.625, 2.5, 5, 10, 20, 40, 80, 160 µM were incubated at 37°C in duplicate with microsomes in 75 mM phosphate buffer without NADPH cofactors. The microsomal protein concentrations in the incubations were 0.25 mg/mL for human and 3.0 mg/mL for the other species. Optimized incubation times in human, rat, monkey and dog were 15, 40, 90 and 120 minutes, respectively, based on conditions of linear formation of M1 from a pilot study (data not shown). The assay was initiated by the addition of substrate (GDC-0834) and terminated by protein precipitation through the addition of acetonitrile containing 0.2 µM internal standard (metoprolol). The formation rate of M1 was measured by LC/MS/MS. Estimation of the maximum rate of M1 formation (V_{max}) and the Michaelis-Menten constant (K_m) was performed by nonlinear regression analysis (GraphPad Prism v.4.03, GraphPad Software; La Jolla, CA, USA) involving fitting of the Michaelis-Menten equation to M1 formation rate (nmol/min/mg protein) versus GDC-0834 concentration (µM) data. Study results were also plotted in Lineweaver-Burke (1/v vs. 1/S) and Eadie-Hofstee (v vs. v/S) plots to assess the presence of more than one enzyme system.

Human Pharmacokinetics Prediction Based on Allometry

Predictions of GDC-0834 clearance (CL) in human were made using simple allometric scaling (Equation 1) and allometric scaling corrected with MLP according to the "Rule of Exponents" (Mahmood and Balian, 1996) (Equations 2 and 3). The volume of distribution at steady state (V_{ss}) was predicted by simple allometric scaling (Equation 4)

$$CL = aW^b \quad (1)$$

$$CL * MLP = aW^b \quad (2)$$

$$MLP = 185.4(BW)^{0.636}(W)^{-0.225} \quad (3)$$

$$V_{ss} = aW^b \quad (4)$$

where a is the allometric coefficient, b is the allometric exponent, W is the body weight in kilogram, BW is the brain weight in kilogram and MLP is the maximum lifespan potential in year.

Clearance Prediction Based on *in vitro/in vivo* Extrapolation (IVIVE)

IVIVE was utilized as another method for human (and animal) clearance prediction. Based on the "Well-Stirred" model (Pang and Rowland, 1977), the following equation (Equation 5) was used for the clearance estimation,

$$CL = \frac{fuCl_{int}Q}{fuCl_{int} + Q} \quad (5)$$

where fu is the GDC-0834 free fraction in blood, Cl_{int} is the intrinsic metabolic clearance based on the *in vitro* $t_{1/2}$ method introduced by Obach et al (1997) from either *in vitro*

liver microsomes (LM) or hepatocytes metabolic stability assays, and Q is the hepatic blood flow.

Phase 1 Clinical Trial of GDC-0834

A clinical double-blind randomized, placebo-controlled, single oral dose study was carried out at Covance Laboratories (Madison, WI, USA). A suspension of GDC-0834 was administered orally after at least an 8-hour fast or a placebo (microcrystalline cellulose) in suspension. Two cohorts of healthy volunteers, based on a 4:2 (Cohort A) and 5:1 (Cohorts B) treatment allocation (GDC-0834:placebo), were given single oral doses of GDC-0834 at 35 and 105 mg, respectively. Blood samples were collected into tubes containing EDTA as an anticoagulant at pre-dose and 0.5, 1, 2, 4, 6, 12, 24 and 48 hours post dose. All subjects remained at the CRO for 48 hours post-dose to evaluate safety and returned on Day 8 (7 days after dosing) for safety evaluation. The decision to escalate to the next dose level was based on a safety review of clinical and laboratory data on all subjects in the previous cohort through Day 3.

Metabolite Identification in Human Urine and Plasma

Urine samples from Cohort B (105 mg) from predose and 4 hours, respectively, were pooled (n = 5). An aliquot (1000 µL) of pooled urine was quenched with 1000 µL acetonitrile followed by vortexing for 5 min and centrifuging for 10 min at 3400 rpm. Plasma samples from 1 to 6 hours from Cohort B were pooled (n = 5). An aliquot (1 mL) of pooled plasma was quenched with 3mL acetonitrile followed by vortexing for 5 min and centrifuging for 10 min. The supernatants were dried down at room temperature with a Labconco Centrivap DNA Concentrator (Kansas City, MS, USA) and reconstituted

with 2:1 H_2O:MeOH. Metabolite identification was performed on reconstituted samples using LC/MS/MS

LC/MS/MS analysis was conducted using a Thermo LTQ XL coupled to an Ultra High Pressure Liquid Chromatograph (UHPLC, Accela Pump), an Accela autosampler, and an Accela PDA (San Jose, CA, USA). The mass spectrometric conditions were set as follows: positive mode ESI, capillary voltage at 17 V, source voltage at 4.5 kV, tube lens voltage at 105 V, capillary temperature at 350ºC, sheath gas flow at 74 units, aux gas flow at 6 units, sweep gas flow at 19 units using full scan and MS^n scan modes. The HPLC column used was a Thermo Hypersil Gold C18 (100 x 2.1 mm, 1.9 µm; Thermo Scientific; Pittsburgh, PA, USA). The solvent system consisted of solvent A (0.1% formic acid in water) and solvent B (0.1% formic acid in acetonitrile). Solvent B was delivered initially at 5%, held for 1 min and increased to 95% via a 25 min gradient, then decreased back to 5% at 26 min, at which time it was retained for 4 min at a flow rate of 400 µL/min with a total run time of 30 min.

Bioanalysis of GDC-0834 and M1 in Preclinical and Clinical Studies

The preclinical samples were prepared for analysis by first aliquoting 25 µL of plasma into a 96 well plate followed by the addition of 25 µL of internal standard solution and 150 µL of acetonitrile to each sample for protein precipitation. The samples were vortexed and centrifuged for 5 min at 10000 rpm. 50 µL aliquots of the resulting supernatant were mixed with 300 µL water and 10 µL was injected onto the LC/MS/MS for analysis. For the clinical samples, a method validated according to US Food and Drug Administration (FDA) guidance for industry on bioanalytical method validation was used where the dynamic range of the assay ranged from 1.0 to 500.0 ng/mL using a 50 µL

aliquot of human plasma for measurement of GDC-0834 and its M1 metabolite (Shin et al., 2011).

Concentrations of GDC-0834 and its M1 metabolite in plasma samples from preclinical species were determined by a non-validated assay using a TSQ quantum liquid chromatography-triple quadrupole mass spectrometer connected to a CTC PAL (Leap Technologies; Chapel Hill, NC, USA) autosampler. GDC-0834 and M1 were separated using a ACE 5 phenyl reverse phase (100x 2.1 mm, 5 µm) column (Advanced Chromatography Technologies; Aberdeen, UK) at room temperature and an LC-10AD pump with a Shimadzu SCL-10A controller (Shimadzu; Columbia, MD, USA). The mobile phase consisted of mobile phase A (water with 0.1% formic acid) and mobile phase B (acetonitrile with 0.1% formic acid). GDC-0834 and M1 metabolite were eluted using an initial condition of 20% mobile phase B followed by a linear gradient to 80% mobile phase B over 5 min with flow rate 0.5 mL/min. The mass spectrometer was in positive-ion mode using an electrospray interface at 400 °C with nitrogen serving as both the nebulizing and heating gas. GDC-0834 and its M1 metabolite were analyzed in the multiple reaction monitoring (MRM) mode using the following transitions *m/z* 597.4 → 127.1 and *m/z* 433.4 → 127.1, respectively. The calibration curves for GDC-0834 and its M1 metabolite were prepared by plotting the appropriate peak area ratios of analyte/internal standard against the known concentrations of GDC-0834 or M1 metabolite in plasma using a linear regression with $1/x^2$ weighing. Concentrations of GDC-0834 and its M1 metabolite in samples were determined by interpolation from their respective standard curves. The dynamic range was 5 to 10000 nM for both parent and metabolite in the preclinical studies. A run was deemed acceptable when quality control

(QC) samples as well as calibration curve samples were within ± 25% of the nominal concentration, except the lowest level of quantification sample where ± 30% was accepted.

DMD Fast Forward. Published on July 8, 2011 as DOI: 10.1124/dmd.111.040840
This article has not been copyedited and formatted. The final version may differ from this version.

RESULTS

PRECLINICAL RESULTS:

Pharmacokinetics of GDC-0834 in Mouse, Rat, Dog and Monkey

Relevant preclinical PK parameters of GDC-0834 are presented in Table 1. The *in vivo* plasma CL is low in rats (4.7 mL/min/kg), moderate in mice and dogs (43 and 14 mL/min/kg, respectively), and high in monkeys (33 mL/min/kg) (Table 1). The volume of distribution at steady state (V_{ss}) is low to moderate (0.25 – 1.5 L/kg) in all species evaluated. The terminal half life ($t_{1/2}$) ranges from 0.158 hr in mouse to 1.09 hr in rat. Oral bioavailability (F) in the mouse, rat, dog, and monkey is 18%, 16%, 32%, and 16%, respectively (Table 1).

Pharmacokinetics of GDC-0834 and M1 Metabolite in PXB and SCID Mouse

Relevant preclinical PK parameters of GDC-0834 in PXB and SCID mice are presented in Table 2. In general, the pharmacokinetics of GDC-0834 was comparable between PXB and SCID mice. Estimates of plasma CL were 22 and 15 mL/min/kg in PXB and SCID mice, respectively (Table 2). The bioavailability (F) in PXB and SCID mice was comparable (35% *vs* 31%, Table 2). Despite these similarities in GDC-0834 PK parameters, PXB mice show a much higher metabolite (M1)/parent ratios compared to SCID mice for both the IV (0.495 *vs* 0.0112) and PO (0.741 *vs* 0.0927) groups (Table 2).

GDC-0834 Metabolic Stability in Liver Microsomes and Hepatocytes

The predicted hepatic CL in liver microsomes (LM) with NADPH are high in all species evaluated (Table 3, upper panel). The elimination of GDC-0834 in human appeared to be due to an NADPH independent pathway as the predicted hepatic CL was similar with and without NADPH in human liver micosomes (Table 3). The contribution

of this pathway appeared to be less prominent in other preclinical species based upon the liver microsome without NADPH data. In hepatocyte stability, clearances are predicted as high in human and monkey and moderate in rat, mouse, and dog (Table 3, middle panel). The *in vivo* preclinical clearances are also listed in the Table 3 (bottom panel) for comparison.

In Vitro and *In Vivo* Metabolite Identification Studies

The *in vitro* hepatocyte metabolism of GDC-0834 is moderate to extensive in all species tested (Table 4). A significant metabolic pathway for GDC-0834 in mouse, rat, dog, monkey and human is amide hydrolysis to form M1 and it is the most pronounced in human hepatocytes. The extent of metabolism to M1 varied according to species being 22%, 8.6%, 12%, 3.6% and 62% in mouse, rat, dog, monkey and human hepatocytes, respectively, based on the peak areas of UV peaks relative to GDC-0834 at the 0 hour time point. Other minor metabolic pathways observed include a combination of oxidation, demethylation, and desaturation of GDC-0834 or metabolite. In cynomolgus monkeys, *N*-demethylation and oxidation are comparable to amide hydrolysis. There were no human-specific metabolites detected in the *in vitro* study (Table 4 and Figure 2).

The amide hydrolysis of GDC-0834 was characterized *in vivo* by measuring concentrations of aniline metabolite, M1 (Figure 1B), in plasma from the PK studies. Consistent with the *in vitro* hepatocyte data (Table 4 and Figure 2), M1 was found in only minor (rat and monkey) to moderate (dog) quantities in plasma from preclinical species dosed orally with GDC-0834 (Figure 3). The metabolite (M1)/parent ratios of exposures were 1.5%, 26% and negligible, respectively, in rats, dogs and monkeys.

DMD Fast Forward. Published on July 8, 2011 as DOI: 10.1124/dmd.111.040840
This article has not been copyedited and formatted. The final version may differ from this version.

Human PK Prediction

Predicted human CL of GDC-0834

Allometric scaling was performed to provide a CL prediction for GDC-0834 in humans using *in vivo* CL estimates from mouse, rat, dog, and monkey PK studies. Predicted clearance in humans was moderate (13 mL/min/kg) based on simple allometric scaling (Figure 4A). Since the allometric exponent (b) is 0.9 ($0.7 < b < 1$), the "Rule of Exponents" (Mahmood and Balian, 1996) was applied. Based on the rule of exponents, the clearance was estimated by allometric scaling corrected using MLP. This resulted in a low predicted clearance of 5.4 mL/min/kg (Figure 4B).

In addition to CL predictions utilizing allometric methods, predictions of human CL were made using *in vitro* methods (Table 3). Human liver micrsomes (HLM) and hepatocytes metabolic stability assays predicted high clearance in humans (~ 19 mL/min/kg, which is close to the human hepatic blood flow).

Predicted human V_{ss} of GDC-0834

Allometric scaling was performed to provide a predicted volume of distribution at steady-state (V_{ss}) of GDC-0834 in humans using estimates of V_{ss} from mouse, rat, dog, and monkey PK studies. Predicted V_{ss} in human was estimated to be 1.4 L/kg (Figure 4C).

CLINICAL RESULTS:

Clinical Human Pharmacokinetics of GDC-0834 and M1

In all subjects dosed with GDC-0834, substantial concentrations of M1 were observed in plasma, whereas levels of GDC-0834 were below the limit of quantitation (< 1 ng/mL) in most plasma samples. At 35 mg, the mean C_{max} and AUC of M1 are 142 ± 48.1 ng/mL and 837 ± 185 hr*ng/mL, respectively (Figure 5A); at 105 mg, the mean C_{max} and AUC of M1 are 390 ± 120 ng/mL and 2448 ± 921 hr*ng/mL, respectively (Figure 5B). The mean C_{max} and AUC of M1 are approximately linear between these two doses. The clinical development of GDC-0834 was terminated based on the above data.

In Vivo Metabolite Identification Studies with GDC-0834

In vivo metabolite identification of plasma and urine from the healthy volunteers dosed with GDC-0834 showed only three metabolites: M1 (amide hydrolysis), and its sequential metabolites M9 (*N*-demethylation), and M10 (oxidation) (Figure 6). Based upon structure assignment by mass spectrometry, M9 and M10 both appear to be metabolites of M1 suggesting that amide hydrolysis was the major metabolic pathway *in vivo* in human.

FORMATION KINETICS of M1:

Results of the enzyme kinetics study of the formation of M1 in rat, dog, monkey and human LM without NADPH are presented in Figure 7. V_{max}, the maximum rate of M1 formation, was substantially higher (21 – 60 fold) in human (0.60 nmol/min/mg protein) compared with that in rat (0.028 nmol/min/mg protein), monkey (0.025 nmol/min/mg protein) and dog (0.010 nmol/min/mg protein) (Figure 7). In contrast, the Michaelis-Menten constant (K_m) was similar among species spanning only an

approximate 3-fold range (22 to 63 μM) (Figure 7). Overall, the estimated intrinsic clearance (V_{max}/K_m) of GDC-0834 from M1 formation was 23 - 169 fold higher in human than that in rat, dog and monkey. The Lineweaver-Burke and Eadie-Hofstee plots for all species studied did not suggest the involvement of more than a single enzyme (data not shown).

DMD Fast Forward. Published on July 8, 2011 as DOI: 10.1124/dmd.111.040840
This article has not been copyedited and formatted. The final version may differ from this version.

DISCUSSION

Species differences in pharmacokinetics (PK) are common and result from differences in physiological processes influencing the absorption, distribution, metabolism and excretion (ADME) of xenobiotics (Lin, 1995; Toutain et al., 2010). One of the major causes of species-dependent PK is species differences in metabolism. It is well known that qualitative and quantitative differences in metabolism exist between humans and other species. As P450 enzymes play an important role in the metabolism of many xenobiotics, advances in the understanding of species differences in P450 structure, substrate specificity and expression have provided much information on the causes of observed differences between humans and preclinical species (Lin, 1995). Comparisons of P450 activities in liver from preclinical species such as mouse, rat, rabbit, dog and micropig show clear differences in activity when compared to human (Bogaards et al., 2000). In fact, despite their genetic similarity to humans, *in vitro* and *in vivo* studies examining P450 activity in non-human primates also indicate differences (Bogaards et al., 2000; Wong et al., 2004). Despite these known differences in the qualitative and quantitative aspects of animal metabolism, preclinical pharmacokinetic studies still serve as an important means to assess human pharmacokinetics and safety of drug candidates prior to clinical studies in human.

The prediction of the human pharmacokinetics of drug candidates is particularly challenging (Beaumont and Smith, 2009). Much literature exists on this particular topic and methodologies available for prediction of human pharmacokinetics are largely either allometric type methods which rely on *in vivo* data, or *in vitro-in vivo* extrapolation (IVIVE) methods which rely heavily on data from *in vitro* studies (Hosea et al., 2009).

The identification of a universal method for the prediction of human pharmacokinetics remains a significant challenge (Hosea, 2011). Allometric methods for prediction of human clearance assume a relationship between clearance and body-weight. These methods work well for compounds where clearance is due to elimination dictated by physiological processes such as blood flow or filtration (Lin, 1998). Therefore, for high clearance compounds where clearance is blood flow-dependent, and compounds that are cleared primarily via the urinary route, allometry should perform reasonably well. However, the rationale of using allometric scaling for human PK prediction has been controversial (Bonate and Howard, 2000) and a known shortcoming of using *in vivo* allometric methods is when there are known species differences in metabolism.

In contrast to allometry, IVIVE methods using *in vitro* data derived from liver fractions apply only to compounds eliminated primarily by the liver. Broad experience with IVIVE methods exists largely for compounds metabolized by P450s (Obach et al., 1997). Literature for IVIVE of compounds metabolized by non-P450 metabolic pathways is much more limited and correlations are not well established for these pathways. As illustrated by the published experience with UDP-glucuronosyltransferases (Miners et al., 2006), IVIVE of substrates of non-P450 enzymes is more problematic. More specific to GDC-0834, there is less known about the enzymes involved in amide hydrolysis. Hydrolysis reactions are not as common as P450 mediated metabolic reactions; however, they play an important role in the metabolism of xenobiotics (Testa and Mayer, 2003). There are a variety of hydrolytic enzymes, including carboxylesterases, cholinesterases, organophosphatases and amidases/peptidases that hydrolyze compounds containing functional groups such as esters, thioesters, amides, and

epoxides. Of these enzymes, cholinesterases and aminopeptidases are probably the most efficient in hydrolyzing the amide bonds of drugs (Uetrecht and Trager, 2007). In addition, carboxylesterases are often active hydrolases in human small intestine and liver and show large species differences in metabolism (Taketani et al., 2007). In preliminary investigations, we performed experiments using hydrolase inhibitors, such as bis-4-nitrophenylphosphate, EDTA and eserine, for class A and B and other hydrolases, and purified hydrolase enzymes, but were unsuccessful in identifying the hydrolytic enzymes responsible for the metabolism of GDC-0834 (data not shown). Finally, to our best knowledge, there is no literature on human clearance prediction methods for compounds like GDC-0834 which appear to be primarily metabolized by amide hydrolysis.

GDC-0834 human clearance predictions using allometric and *in vitro* methodologies resulted in a wide range of values (5.4 – 19 mL/min/kg). As discussed, the metabolism of GDC-0834 was species dependent in terms of both rate and metabolic pathway. As such, we had low confidence in our GDC-0834 human clearance predictions estimated using allometric methods. In addition, there appeared to be a lack of IVIVE in preclinical species with predictions of clearance using microsomes being higher than observed *in vivo* clearance in rat, mouse and dog. IVIVE improved when hepatocyte data were used; however, predictions of clearance in the rat by IVIVE were still higher than observed *in vivo*. Furthermore, our overall understanding of amide hydrolysis enzymes is considerably less than for P450s and there is no literature on the IVIVE of compounds metabolized by amide hydrolysis. Given these challenges, our confidence in the IVIVE clearance prediction were equally low. Recently, a chimeric mouse model with a humanized liver designated as the PXB mouse, has been developed

and characterized for the drug discovery (Tateno et al., 2004; Kikuchi et al., 2010). We attempted to retrospectively evaluate this model in order to determine if it could have been used as an *in vivo* tool to elucidate the pharmacokinetic behavior of GDC-0834 in humans. It should be recognized that the utility of PXB mice as a useful tool for understanding drug metabolism in humans has been largely studied using compounds metabolized primarily by P450 (Kikuchi et al., 2010). Qualitatively, our studies with PXB mouse show a higher level of the amide hydrolysis metabolite consistent with *in vitro* data from human liver microsomes and hepatocytes. However, quantitatively, there appeared to be a significant difference between GDC-0834 clearance in PXB mice (low clearance) and what was observed in humans. Moreover, the clearance was similar between PXB and control SCID mice. Clearly, additional tools are required to better understand the IVIVE of compounds metabolized by amide hydrolysis.

Additional *in vitro* enzyme kinetics studies were conducted to understand the species differences in the amide hydrolysis of GDC-0834. The results of these studies show that human liver has a much greater capacity (i.e. higher V_{max}) for amide hydrolysis of GDC-0834 suggesting a higher expression/activity of the enzymes involved in the amide hydrolysis reaction in humans. These findings were consistent with observations from the human pharmacokinetic study where there was little to no parent compound detected in human plasma following oral dosing (Figure 5). Observed metabolites in human plasma and urine samples from this study were all sequential metabolites of the primary amide hydrolysis metabolite, M1 (Figure 6). In addition, incubations using intestinal S9 fraction suggested GDC-0834 exhibited little to no intestinal metabolism and GDC-0834 was found to be chemically stable in simulated gastric fluid with and

without pepsin over a period of 2 hours (personal communication). Furthermore, a blood stability assay indicated GDC-0834 was stable for 3 hours in human blood. Collectively, the *in vitro* and *in vivo* data suggest that in humans absorbed GDC-0834 is converted primarily to the M1 metabolite via a first pass effect by the liver. Recently, species differences in amide hydrolysis have been reported for an agonist of the bile acid Takeda G-protein-coupled receptor 5 (TGR5) (Eng et al., 2010). The TGR5 agonist being investigated behaved differently than GDC-0834 and underwent amide bond cleavage in both rat and mouse plasma. In contrast with the findings in rodents, the TGR5 agonist was resistant to hydrolytic cleavage in both dog and human plasma (Eng et al., 2010). Our understanding of species differences in amide hydrolysis will continue to grow as more examples of this metabolic route are observed and reported.

Rheumatoid arthritis (RA) is an autoimmune disease that causes chronic inflammation of the joints, the tissues that surround the joints, and other organs in the body. The current standard of care for RA is methotrexate which is not without its shortcomings, including a number of potentially serious adverse effects, such as haematopoietic suppression, hepatotoxicity and pulmonary toxicity (Stamp et al., 2006). Based upon the properties of current therapies, there is a clear need for newer and safer therapies for RA. GDC-0834 is a potent and selective BTK inhibitor with an acceptable preclinical toxicity profile and demonstrated preclinical efficacy in the rat CIA model (Liu et al., 2011). The major liability for GDC-0834 was the low confidence in our human clearance predictions. Approaches to elucidate human pharmacokinetics more rapidly with reduced cost include the use of micro-dosing studies (Lappin, 2010). In our case, we conducted single dose toxicology studies to support the submission of a single

dose investigational new drug application (IND). A single dose IND enabled a rapid assessment of the human pharmacokinetics of GDC-0834, resulting in the termination of GDC-0834 under a shorter time-frame and with a reduced cost than if we chose to evaluate the compound under a traditional IND. Finally, the results from *in vitro* studies with liver microsomes and hepatocytes appeared to correlate with the *in vivo* situation in humans, suggesting an *in vitro* to *in vivo* correlation for amide hydrolysis. Information gathered using GDC-0834 greatly helped in our design of molecules that are void of this liability.

DMD Fast Forward. Published on July 8, 2011 as DOI: 10.1124/dmd.111.040840
This article has not been copyedited and formatted. The final version may differ from this version.

ACKNOWLEDGMENTS

We thank the BTK team members at Genentech and CGI Pharmaceuticals Inc., and the staff at Department of DMPK for their contributions in generating the data for this manuscript.

DMD Fast Forward. Published on July 8, 2011 as DOI: 10.1124/dmd.111.040840
This article has not been copyedited and formatted. The final version may differ from this version.

AUTHORSHIP CONTRIBUTIONS

Participated in research design: Liu, Halladay, Shin, S Wong, Coraggio, La, Baumgardner, Le, Gopaul, Boggs, Kuebler, Davis, Liao, Lubach, Deese, Sowell, Currie, Young, Khojasteh, Hop and H Wong.

Conducted experiments: S Wong, Coraggio, La, Baumgardner, Le, Gopaul, Davis, Lubach, Deese, Sowell, and Currie.

Performed data analysis: Liu, Halladay, S Wong, Coraggio, La, Baumgardner, Le, Gopaul, Boggs, Kuebler and H Wong.

Wrote or contributed to the writing of the manuscript: Liu, Halladay, Shin, Lubach, Currie, Young, Khojasteh, Hop and H Wong.

REFERENCES

Beaumont K and Smith DA (2009) Does human pharmacokinetic prediction add significant value to compound selection in drug discovery research? *Curr Opin Drug Discov Devel* **12:** 61-71.

Bogaards JJ, Bertrand M, Jackson P, Oudshoorn MJ, Weaver RJ, van Bladeren PJ, and Walther B (2000) Determining the best animal model for human cytochrome P450 activities: a comparison of mouse, rat, rabbit, dog, micropig, monkey and man. Xenobiotica **30:** 1131-1152.

Bonate PL and Howard D (2000) Prospective allometric scaling: does the emperor have clothes? *J Clin Pharmacol* **40:** 335-340.

Brunner C, Müller B, and Wirth T (2005) Bruton's Tyrosine Kinase is involved in innate and adaptive immunity. *Histol Histopathol* **20:** 945-955.

Di Paolo JA, Huang T, Balazs M, Barbosa J, Barck KH, Bravo BJ, Carano RAD, Darrow J, Davies DR, DeForge LE, Diehl L, Ferrando R, Gallion SL, Giannetti AM, Gribling P, Hurez V, Hymowitz SG, Jones R, Kropf JE, Lee WP, Maciejewski PM, Mitchell SA, Rong H, Staker BL, Whitney JA, Yeh S, Young WB, Yu C, Zhang J, Reif K, and Currie KS (2011) Specific Btk inhibition suppresses B-cell and myeloid-cell mediated arthritis. *Nat Chem Biol* **7:** 41-50.

Eng H, Niosi M, McDonald TS, Wolford A, Chen Y, Simila ST, Bauman JN, Warmus J, and Kalgutkar AS (2010) Utility of the carboxylesterase inhibitor bis-para-nitrophenylphosphate (BNPP) in the plasma unbound fraction determination for a

hydrolytically unstable amide derivative and agonist of the TGR5 receptor. *Xenobiotica* **40:** 369-380.

Hosea NA (2011) Drug design tools - in silico, in vitro and in vivo ADME/PK prediction and interpretation: is PK in monkey an essential part of a good human PK prediction? *Curr Top Med Chem* **11:** 351-357.

Hosea NA, Collard WT, Cole S, Maurer TS, Fang RX, Jones H, Kakar SM, Nakai Y, Smith BJ, Webster R, and Beaumont K (2009) Prediction of human pharmacokinetics from preclinical information: comparative accuracy of quantitative prediction approaches. *J Clin Pharmacol* **49:** 513-533.

Khan WN, Alt FW, Gerstein RM, Malynn BA, Larsson I, Rathbun G, Davidson L, Müller S, Kantor AB, Herzenberg LA, Rosen FS, and Sideras P (1995) Defective B cell development and function in Btk-deficient mice. *Immunity* **3:** 283-299.

Kikuchi R, McCown M, Olson P, Tateno C, Morikawa Y, Katoh Y, Bourdet DL, Monshouwer M, and Fretland AJ (2010) Effect of hepatitis C virus infection on the mRNA expression of drug transporters and cytochrome p450 enzymes in chimeric mice with humanized liver. *Drug Metab Dispos* **38:** 1954-1961.

Lappin G (2010) Microdosing: current and the future. *Bioanalysis* **2:** 509-517.

Lin JH (1995) Species similarities and differences in pharmacokinetics. *Drug Metab Dispos* **23:** 1008-1021.

Liu L, Paolo JD, Barbosa J, Rong H, Reif K, and Wong H (2011) Anti-arthritis effect of GDC-0834, a novel Bruton's tyrosine kinase inhibitor, in rat collagen-induced arthritis model and mechanism-based pharmacokinetic/pharmacodynamic modeling: relationships between pBTK inhibition and efficacy. *J Pharmacol Exp Ther* **338:** 154-163.

Mahmood I and Balian JD (1996) Interspecies scaling: predicting clearance of drugs in humans. Three different approaches. *Xenobiotica* **26:** 887–895.

Miners MO, Knights KM, Houston BJ and Mackenzie PI (2006) In vitro–in vivo correlation for drugs and other compounds eliminated by glucuronidation in humans: Pitfalls and promises. *Biochem Pharmacol.* **71:** 1531-1539

Niiro H and Clark EA (2002) Regulation of B-cell fate by antigen-receptor signals. *Nat Rev Immunol* **2:** 945–956.

Obach RS, Baxter JG, Liston TE, Silber BM, Jones BC, MacIntyre F, Rance DJ, Wastall P (1997) The prediction of human pharmacokinetic parameters from preclinical and in vitro metabolism data. *J Pharmacol Exp Ther* **283**: 46-58.

Pan Z (2008) Bruton's tyrosine kinase as a drug discovery target. *Drug News Perspect* **21:** 357-362.

Pan Z, Scheerens H, Li SJ, Schultz BE, Sprengeler PA, Burrill LC, Mendonca RV, Sweeney MD, Scott KC, Grothaus PG, Jeffery DA, Spoerke JM, Honigberg LA, Young PR, Dalrymple SA, and Palmer JT (2007) Discovery of selective irreversible inhibitors for Bruton's tyrosine kinase. *ChemMedChem* **2:** 58-61.

Pang KS and Rowland M (1977) Hepatic clearance of drugs. I. Theoretical considerations of a "well-stirred" model and a "parallel tube" model. Influence of hepatic blood flow, plasma and blood cells binding, and the hepatocellular enzymatic activity on hepatic drug clearance. *J Pharmacokinet Biopharm* **5:** 625-653.

Satterthwaite AB and Witte ON (2000) The role of Bruton's tyrosine kinase in B-cell development and function: a genetic perspective. *Immunol Rev* **175:** 120-127.

Sharma S, Orlowski G, and Song W (2009) Btk regulates B cell receptor-mediated antigen processing and presentation by controlling actin cytoskeleton dynamics in B cells. *J Immunol* **182:** 329-339.

Shin YG, Jones SA, Murakami SC, Liu L, Wong H, Buonarati MH, and Hop CECA (2011) Validation and application of a liquid chromatography-tandem mass spectrometric method for the determination of GDC-0834 and its metabolite in human plasma using semi-automated 96-well protein precipitation. (In press)

Stamp L, Roberts R, Kennedy M, Barclay M, O'Donnell J, and Chapman P (2006) The use of low dose methotrexate in rheumatoid arthritis - are we entering a new era of therapeutic drug monitoring and pharmacogenomics? *Biomed Pharmacother* **60:** 678-687.

Taketani M, Shii M, Ohura K, Ninomiya S, and Imai T (2007) Carboxylesterase in the liver and small intestine of experimental animals and human. *Life Sci* **81:** 924-932.

Tateno C, Yoshizane Y, Saito N, Kataoka M, Utoh R, Yamasaki C, Tachibana A, Soeno Y, Asahina K, Hino H, Asahara T, Yokoi T, Furukawa T, and Yoshizato K (2004) Near

completely humanized liver in mice shows human-type metabolic responses to drugs. *Am J Pathol* **165:** 901–912.

Testa B and Mayer JM (2003) *Hydrolysis in drug and prodrug metabolism: chemistry, biochemistry, and enzymology*, 1st ed. Wiley-VCH, Weinheim, Germany.

Toutain PL, Ferran A, and Bousquet-Mélou A (2010) Species differences in pharmacokinetics and pharmacodynamics. *Handb Exp Pharmacol* **199:** 19-48.

Uckun FM, Tibbles HE, and Vassilev AO (2007) Bruton's tyrosine kinase as a new therapeutic target. *Anticancer Agents Med Chem* **7:** 624-632.

Uetrecht JP and Trager W (2007) *Drug Metabolism: Chemical and Enzymatic Aspects*, 1st ed. Informa Healthcare, New York.

Wong H, Grossman SJ, Bai SA, Diamond S, Wright MR, Grace JE Jr., Qian M, He K, Yeleswaram K, and Christ DD (2004) The chimpanzee (Pan troglodytes) as a pharmacokinetic model for selection of drug candidates: Model characterization and application. *Drug Metab Disp* **32:** 1359-1369.

FOOTNOTES

This work was partially presented as an abstract (P361) at the *9th international ISSX meeting;* 2010 September 4 – 8; Istanbul Turkey.

Current address: Gilead Sciences, 36 East Industrial Road, Branford, CT, 06405, USA (K.S.C.)

Send reprint requests to: Dr. Lichuan Liu, Genentech, Inc., MS# 412A, 1 DNA Way, South San Francisco, CA 94080. E-mail: liu.lichuan@gene.com

DMD Fast Forward. Published on July 8, 2011 as DOI: 10.1124/dmd.111.040840
This article has not been copyedited and formatted. The final version may differ from this version.

LEGENDS FOR FIGURES

Figure 1. The structures of GDC-0834 (A) and its aniline metabolite M1 (B).

Figure 2. The proposed metabolic pathway of GDC-0834 in cryopreserved hepatocytes of the mouse (M), rat (R), dog (D), cyno (C, interchangeable with monkey in this paper), and humans following incubation with GDC-0834 for 3 Hours. M1 is the aniline metabolite, which constitutes 62% in human hepatocytes based on peak areas of UV peaks relative to the parent compound (GDC-0834) at the 0 hour time point.

Figure 3. The plasma PK profiles of GDC-0834 (solid dots) and its aniline metabolite M1 (empty dots) in rats (A), dogs (B) and monkeys (C) dosed orally at 5 mg/kg. The metabolite/parent ratios of exposures are 1.5%, 26% and negligible, respectively, in rats, dogs and monkeys.

Figure 4. The allometric scaling of human clearance (CL) and volume of distribution at steady state (V_{ss}) based on the preclinical *in vivo* mouse, rat, monkey and dog PK data. The predicted human clearances are 13 and 5.4 mL/min/kg, respectively, based on the simple allometry (A) and allometry corrected with maximum life span (MLP) (B); the predicted human V_{ss} is 1.4 L/kg (C).

Figure 5. The pharmacokinetic profiles of M1, metabolite of GDC-0834, dosed at (A) 35 mg (n = 4) and (B) 105 mg (n = 5) in the healthy volunteers. The mean C_{max} and AUC of M1 are approximately linear between two doses. There is no observed parent (GDC-0834) concentration in the plasma in both cohorts.

Figure 6. The *in vivo* metabolite identification of plasma and urine from the healthy volunteers dosed with GDC-0834. Only M1 and its derivative metabolites were observed.

Figure 7. An enzyme kinetic study, by monitoring M1 formation, was carried out in human (A), rat (B), monkey (C) and dog (D) liver microsomes without NADPH. The data demonstrated it was mainly V_{max} but not K_m that caused the significant amide hydrolysis in human compared with other species. The intrinsic clearance ($Cl_{int} = V_{max}/K_m$) in human is 23 – 169 fold higher than that in rat, monkey and dog.

DMD Fast Forward. Published on July 8, 2011 as DOI: 10.1124/dmd.111.040840
This article has not been copyedited and formatted. The final version may differ from this version.

Table 1 Pharmacokinetics (mean ± SD) of GDC-0834 in CD-1 mice, Sprague-Dawley rats, Beagle dogs, and Cynomolgus monkeys.

Parameters	Mouse [a]	Rat [b]	Dog [c]	Monkey [d]
IV Administration				
No. of animals	24 (3/timepoint)	3	3	3
Sex	Female	Male	Male	Male
Dose (mg/kg)	1	1	1	1
CL (mL/min/kg)	43.0	4.66±4.81	13.6±2.34	32.7±3.06
$t_{1/2}$ (hr)	0.158	1.09±0.503	0.789±0.0705	0.615±0.0548
MRT (hr)	0.156	1.29±0.579	0.933±0.0907	0.745±0.131
V_{ss} (L/kg)	0.402	0.253±0.129	0.755±0.0655	1.46±0.312
Renal clearance (mL/min/kg)	NA [e]	NA [e]	NA [f]	0.00127 [g]
Oral Administration				
No. of animals	24 (3/timepoint)	3	3	3
Sex	Female	Male	Male	Male
Dose (mg/kg)	5	5	5	5
C_{max} (ng/mL)	351	1330±494	651±128	198±46.0
t_{max} (hr)	0.500	1.33±0.577	0.750±0.433	1.33±0.577
$AUC_{0-\infty}$ (ng • hr/mL)	348	5310±1340	1990±660	393±89.1
F (%)	17.9	16.1±4.06	31.9±10.6	15.5±4.23

$AUC_{0-\infty}$ = area under the concentration–time curve, extrapolated to infinity; CL = plasma clearance; C_{max} = highest observed plasma concentration; F = bioavailability; IV = intravenous; MCT = 0.5% weight-to-volume ratio methylcellulose with 0.2% volume to volume ratio polysorbate 80 in water; MRT = mean residence time; NA = not available; PEG = polyethylene glycol; $t_{1/2}$ = half-life; t_{max} = time to maximum concentration; V_{ss} = volume of distribution at steady state.

[a] Oral data were from GDC-0834 dosed orally as solution (free base) in 20% cremophor EL/10% ethyl alcohol.

[b] Oral data were from GDC-0834 dosed orally as crystalline suspension (free base) in MCT.

[c] Oral data were from GDC-0834 dosed orally as crystalline suspension (free base) in MCT after pretreatment with pentagastrin.

[d] Oral data were from GDC-0834 dosed orally as solution (free base) in 60% PEG 400.

[e] No urine was collected.

[f] Data were not reportable.

[g] Renal clearance was assessed for the IV group only.

DMD Fast Forward. Published on July 8, 2011 as DOI: 10.1124/dmd.111.040840
This article has not been copyedited and formatted. The final version may differ from this version.

Table 2 Pharmacokinetics of GDC-0834 and M1 in PXB and SCID mice.

Treatment	Analyte	$AUC_{0-\infty}$ (hr*uM)	CL (mL/min/kg)	V_{ss} (L/kg)	M1:Parent AUC Ratio
PXB IV	GDC-0834	1.30	21.5	0.507	NA
	M1	0.644	NA	NA	0.495
SCID IV	GDC-0834	1.83	15.3	0.435	NA
	M1	0.0205	NA	NA	0.0112
			F		
PXB PO	GDC-0834	2.28	35%	NA	NA
	M1	1.69	NA	NA	0.741
SCID PO	GDC-0834	2.88	31%	NA	NA
	M1	0.267	NA	NA	0.0927

$AUC_{0-\infty}$ = area under the concentration–time curve, extrapolated to infinity; CL = plasma clearance; F = bioavailability; IV = intravenous; NA = not available; PO=oral; V_{ss} = volume of distribution at steady state.

DMD Fast Forward. Published on July 8, 2011 as DOI: 10.1124/dmd.111.040840
This article has not been copyedited and formatted. The final version may differ from this version.

Table 3 The predicted clearances (CL) in liver microsomes (LM, with and without NADPH) and hepatocytes for human, rat, mouse, dog and monkey. The human clearance is predicted as high under all conditions. For the preclinical species, the clearance is predicted as low in LM without NADPH. The *in vivo* clearance is low in rats, moderate in mice and dogs, and high in monkeys.

	Predicted CL_{hep} (mL/min/kg)				
	Human	**Rat**	**Mouse**	**Dog**	**Monkey**
Liver Microsomes					
with NADPH	**19**	**39**	**79**	**28**	**36**
without NADPH	**18**	**7.8**	**25**	**6.8**	**2.4**
Hepatocytes	**19**	**25**	**63**	**19**	**32**
In vivo CL (mL/min/kg)	**-**	**4.7**	**43**	**14**	**33**

DMD Fast Forward. Published on July 8, 2011 as DOI: 10.1124/dmd.111.040840
This article has not been copyedited and formatted. The final version may differ from this version.

Table 4 Percent of unchanged GDC-0834 and metabolites formed by incubation of 10 μM of GDC-0834 in cryopreserved hepatocytes of the mouse, rat, dog, cyno (monkey), and humans for 3 hours.

Analyte	Retention Time (min)	M	R	D	C	H	Biotransformation Pathway
GDC-0834	22.6	44.1	79.5	83.1	46.5	19.9	—
M1	9.1	22.3	8.6	12.2	3.6	61.5	Amide Hydrolysis
M2	13.0	1.1	0.4	0.4	0.4	1.2	Oxidation
M3	18.2	2.8	3.1	2.0	8.6	0.3	N-demethylation
M4	6.56	1.8	ND	1.2	ND	ND	Amide Hydrolysis + N-demethylation
M5	14.1	2.8	0.7	1.3	0.7	2.6	Desaturatrion
M6	20.2	2.2	ND	4.3	ND	ND	N-Demethylation
M7	20.3	ND	ND	ND	5.1	ND	Oxidation
M8	21.2	ND	3.3	ND	ND	ND	Oxidation

C = male cynomolgus monkey hepatocytes; D = male beagle dog hepatocytes; H = pooled human hepatocytes; M = mouse hepatocytes; ND = not detected; R = rat hepatocytes

Note: Percent composition is semi-quantitative and is based on peak areas of UV peaks and calculated relative to the parent compound (GDC-0834) at the 0-hour time point.

DMD Fast Forward. Published on July 8, 2011 as DOI: 10.1124/dmd.111.040840
This article has not been copyedited and formatted. The final version may differ from this version.

Figure 1

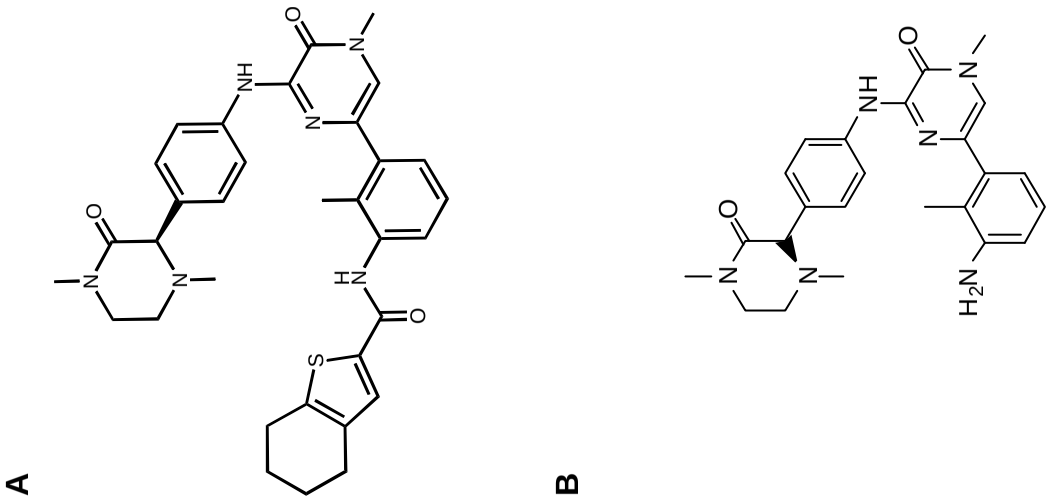

Figure 2

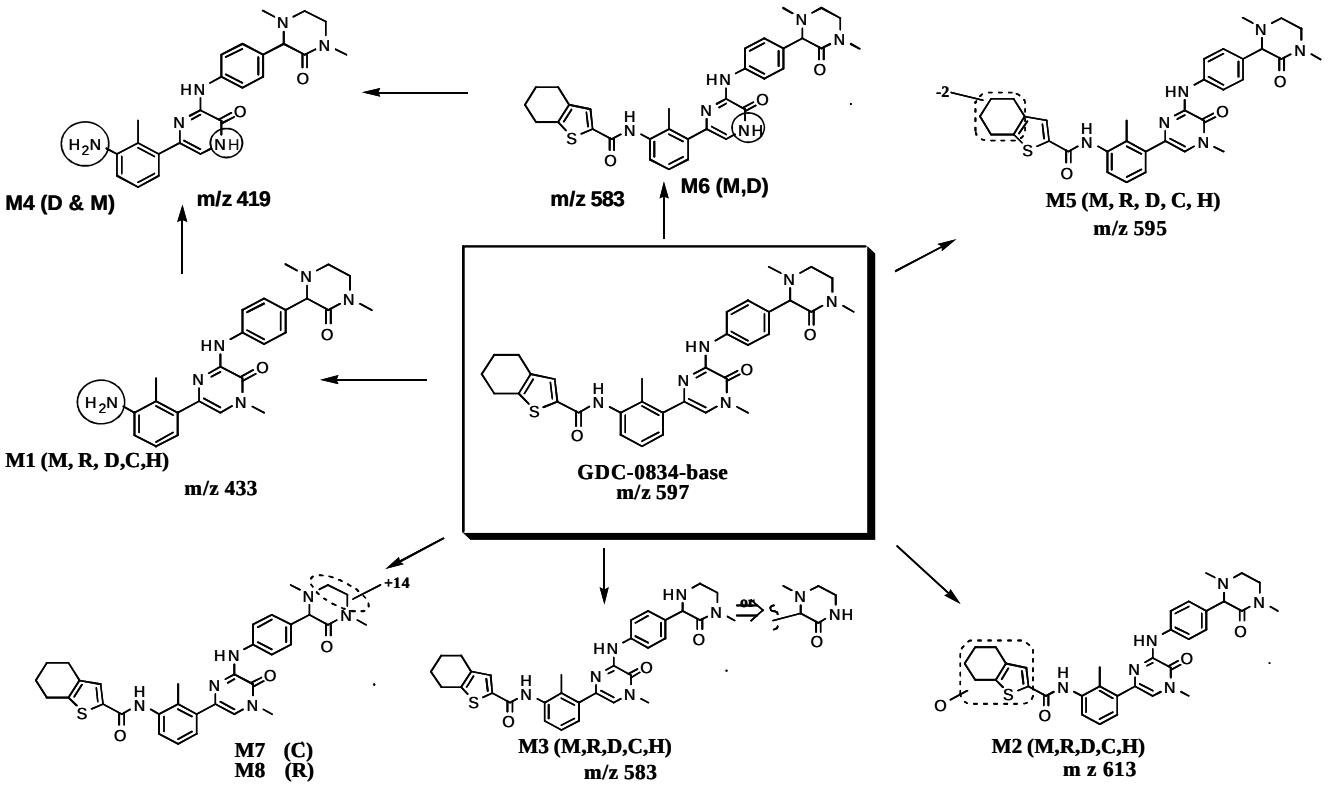

Figure 3

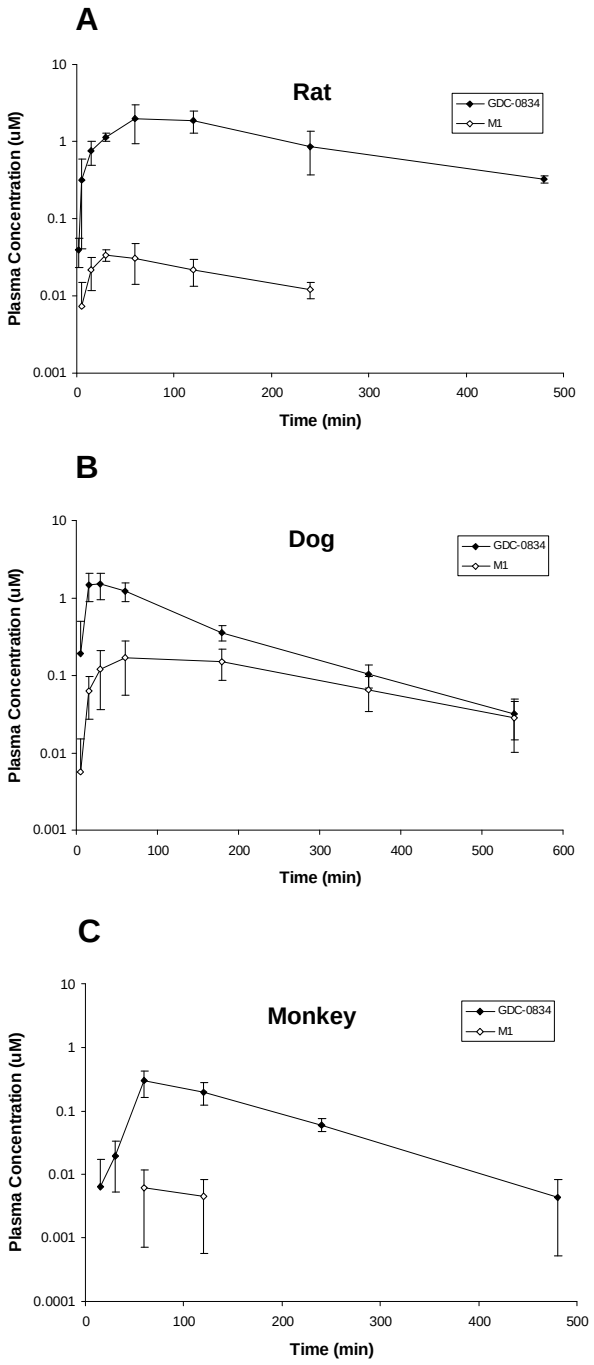

Figure 4

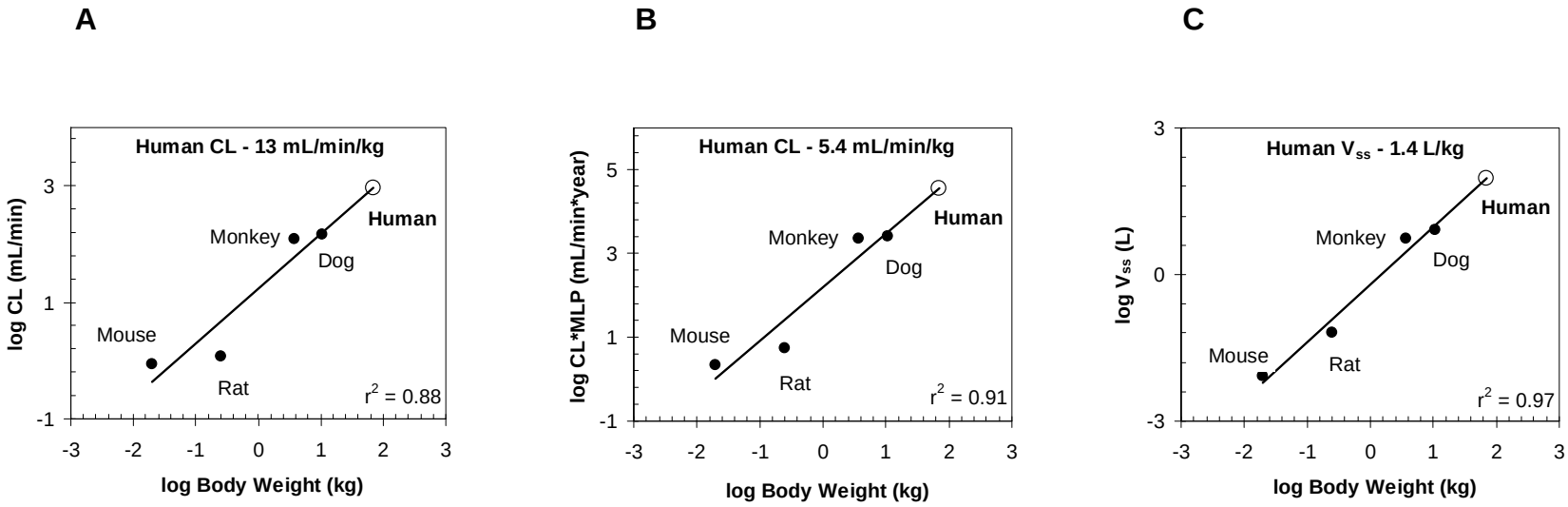

Figure 5

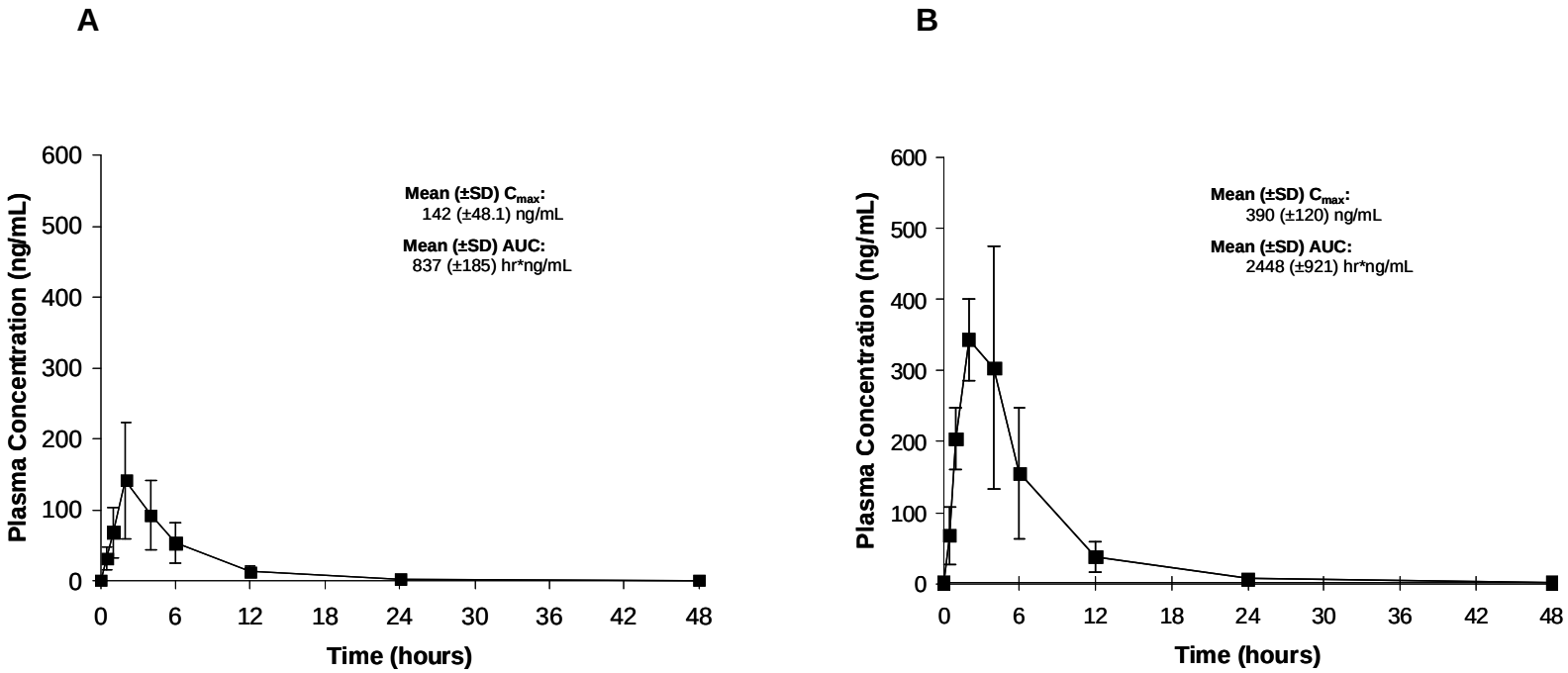

DMD Fast Forward. Published on July 8, 2011 as DOI: 10.1124/dmd.111.040840
This article has not been copyedited and formatted. The final version may differ from this version.

Figure 6

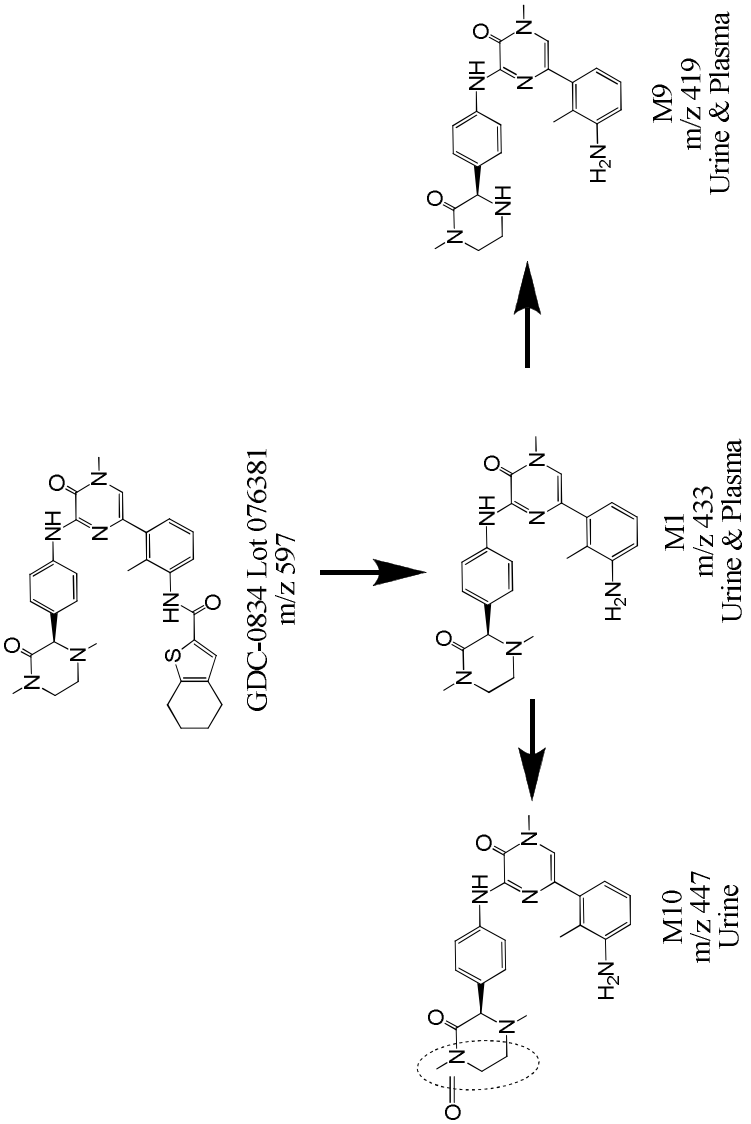

Figure 7